BALKAN JOURNAL OF ELECTRICAL & COMPUTER ENGINEERING, Vol. 12, No. 1, March 2024

Research Article

Design and analysis of L and LCL filters for grid-connected HNPC inverters used in renewable energy systems

Muhammet Cengiz, Turgay Duman

***Abstract*—With the widespread integration of renewable energy systems (RES) into the electric grid, maintaining power quality within specified limits has become a major focus. The total harmonic distortion (THD) value of the currents transferred to the grid and directly affecting power quality in RES such as grid-connected photovoltaic (PV) and fuel cells (FC) should not exceed 5%. To achieve this objective, various filter topologies are used to interface between the inverters, which are components of PV and FC systems, and the grid. Although there are numerous filter topologies, L and LCL-type passive filters are the most commonly used topologies in grid-connected systems. This study analyzes the L and LCL-type filter topologies for the H-bridge neutral point clamped (HNPC) inverter. Using MATLAB/Simulink®, a simulation of a 3 kW system employing L and LCL filters has revealed THD values of 1.56% and 0.07% for grid currents, respectively. Additionally, the HNPC inverter's efficiency has been determined at 98.46% in the LCL filter configuration. This study has been focused on modeling and comparing simulation results to investigate the harmonic attenuation capabilities of L and LCL filters, assess the maximum power transferred to the grid, and analyze their impact on grid currents.**

***Index Terms*—HNPC inverter, L and LCL filters, power quality, PV system, sliding mode controller.**

I. Introduction

ELECTRICAL energy, which constitutes approximately 20% of the global total energy consumption, is being demanded more and more each day, and it is expected that the total electrical energy demand will increase by more than 80% by 2050 [1]. Considering the reduction of traditional energy sources (coal, oil, etc.) used in energy production and the damage they cause to the environment, energy consumption is a major concern of today's society, and alternative energy sources are needed. Renewable energy technologies, particularly photovoltaic and fuel cell systems that generate clean and sustainable electricity from renewable energy sources such as solar, wind, and hydrogen, are regarded as one of the most important future solutions [2]. According to the reports issued by the International Energy Agency (IEA) and the International Renewable Energy Agency (IRENA), renewable sources are projected to contribute more than 80% to the overall energy production worldwide by 2050. Furthermore, it is anticipated that the proportion of solar energy in total electricity production will increase to approximately 25%, and the percentage of hydrogen energy in total energy consumption will rise to around 13% [1], [3], [4].

PV and FC systems can generally be classified into two groups: grid-connected and stand-alone. Grid-connected PV (GCPV) systems are decentralized (distributed) power systems that can operate in parallel with the electricity transmission and distribution grid [5]. Parallel operation with the grid is the transfer of the power produced in excess of the needs of the loads in the system back to the electricity grid. Therefore, in contrast to standalone systems, GCPV systems do not need additional storage devices like battery packs, which lowers the cost of the system and makes it easier to maintain and reinstall [6], [7]. Furthermore, GCPV systems account for the vast majority of installed PV capacity when compared to stand-alone systems. Similarly, grid-connected FC systems (GCFC) are an important part of research and are widely discussed in areas such as air conditioning, electromechanical systems, lighting, and electronic devices [8]. To ensure the electrical grid's power quality, the more widely used GCPV and GCFC systems must meet certain specifications. The most important specification is to transfer a sinusoidal current to the grid with a total harmonic distortion value of no more than 5% [9], [10]. PV panels and FCs generate DC voltage. Fig. 1 depicts the overall grid connection structure of both systems.

Although the DC voltage generation logic of both sources differs, the components and power conversion principles required for grid integration are similar [2], [8]. To transfer a sinusoidal current from PV and FC systems to the grid, an inverter is required to convert the DC power produced by PV panels or fuel cells into AC power with a specific frequency and amplitude. Therefore, inverters are a critical component of RES such as PV and FC. Various inverter topologies used in PV applications have been presented in the literature [7]. Among these topologies, the HNPC inverter is widely used in grid-connected applications due to its advantages such as low THD, transformerless operation, high quality power conversion, and operation at high input voltages with low-capacity switches [11], [12]. On the other hand, grid-connected inverters modulated with pulse width modulation (PWM) techniques contain switching harmonic components in their output waveforms [13]. Therefore, inverters must be connected to the grid via a filter to provide sinusoidal current to the grid without harmonic distortion. Generally, three basic filter topologies are used at the inverter output, namely L, LC,

Muhammet Cengiz is with the Department of Electrical and Electronic Engineering, Engineering and Architecture Faculty, Erzurum Technical University, Erzurum, 25050, Turkey e-mail: muhammet.cengiz@erzurum.edu.tr

Turgay Duman is with the Department of Electrical and Electronic Engineering, Engineering and Architecture Faculty, Erzurum Technical University, Erzurum, 25050, Turkey e-mail: turgay.duman@erzurum.edu.tr

Manuscript received July 8, 2023; accepted Jan 21, 2024.
DOI: 10.17694/bajece.1324513

Copyright © BAJECE ISSN: 2147-284X https://dergipark.org.tr/bajece

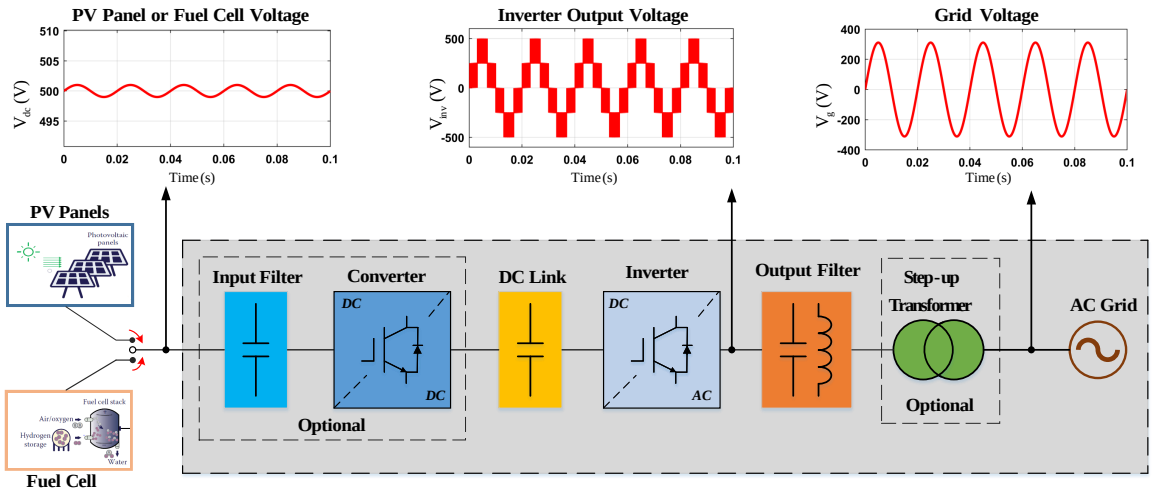

Fig. 1. General structure of grid connected system (PV or FC).

and LCL.

When selecting a suitable filter topology for grid -connected inverters, it is necessary to consider parameters such as size, cost, filter losses, and dynamic system properties, as well as effectively reducing harmonics [14]. The L filter contains only one component, which makes it have a simple topology and easy to design. However, it requires a very high inductance value for applications above a few kilowatts [15]. Using a high inductance value can make the system cumbersome and expensive, and it may also increase the filter's losses. Additionally, the system's dynamic response can be poor due to long voltage drops in the filter [16], [17]. The LC and LCL filter topologies are used to mitigate the disadvantages of using the L filter in high-capacity systems, such as size, cost, losses, and poor system dynamics. By increasing the capacitor value in the LC filter, the inductance value is decreased, and thus the disadvantages of the L filter mentioned above can be mitigated. However, in grid-connected systems, a high capacitor value is not quite preferred because it can cause problems such as sudden current peaks, grid side resonance due to reactive power requirements, and reliance on grid impedance for harmonic attenuation [17]. Therefore, L and LCL-type filter topologies are generally used in grid-connected systems [18], [19], [20].

LCL filters offer advantages over L filters such as improved harmonic performance, as well as lower size and cost [15], [21]. In addition, LCL filters are among the most widely used topologies in grid-connected inverters due to their advantages, such as lower ripple in the current injected into the grid and operating at a lower switching frequency [19]. However, LCL filters may suffer from resonances that occur due to reactive power requirements and must be damped to ensure system stability. Two types of damping methods, passive and active, are generally used to alleviate the resonance problem. The passive damping method can be implemented by adding a damping resistor in series with the LCL filter capacitor [21]. Although this method is simple, it reduces the harmonic attenuation performance of the LCL filter by causing additional power losses due to the added resistance [20]. The active damping method is based on the concept of an imaginary resistor connected to the current control loop to eliminate power loss [22]. Although the imaginary resistor concept provides better harmonic attenuation performance, it increases control complexity and requires the use of an additional set of sensors. On the other hand, the active damping effect can also be achieved by controlling the grid current without the use of imaginary resistance [23]. The sliding mode control (SMC) method, which is used in grid current control and has advantages such as reducing control complexity, robustness against parameter changes, fast dynamic response, and ease of application, also overcomes the resonance problem without the need for additional damping methods [19], [20], [23].

This article is structured as follows: Section 2 gives an overview of the HNPC structure and control for single-phase grid connection. Sections 3 and 4 discuss the design phases of the L and LCL filters, respectively, and provide guidelines for determining filter component values. Section 5 presents simulation results for the grid connection states of L and LCL filters. Lastly, Section 6 presents the conclusions.

II. Single-phase grid-connected HNPC inverter

Power electronic devices, such as DC-DC converters and DC-AC inverters, must be used to transfer the DC power generated by the PV panel or FC to the electrical grid as maximum AC power. In recent years, researchers have focused on single-stage power processing systems that use only inverters as power converters, both to improve the overall efficiency of PV systems and to increase the power density of the inverters [24]. The single-phase grid-connected inverter block diagram of the system is shown in Fig. 2.

As depicted in Fig. 2, the HNPC inverter enables power transfer between the grid and the PV panel. The PV panel is treated as a constant DC source to simplify the system. The HNPC inverter is made up of two 3-level NPC inverter legs connected in parallel. Each NPC leg generates three different voltage levels at the output: $-V_{dc}/2$, $+V_{dc}/2$, and

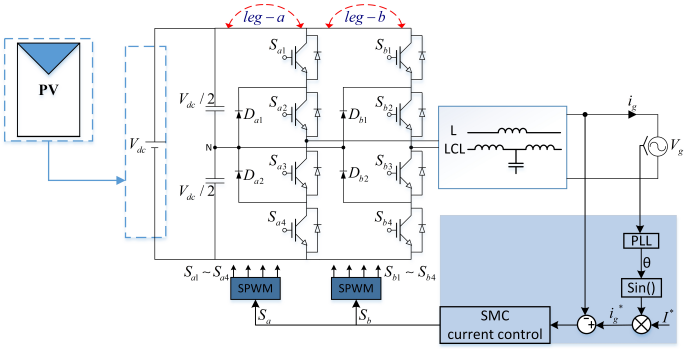

Fig. 2. The single-phase grid-connected HNPC inverter.

zero. Parallel connection of the NPC inverter legs results in the generation of five different voltage levels at the HNPC inverter output: $-V_{dc}, +V_{dc}, 0, -V_{dc}/2, +V_{dc}/2$. The switching states and voltage levels for the HNPC are given in Table 1. This inverter topology and suitable switching states have been discussed in the previous study [25].

TABLE I
SWITCHING STATES OF THE HNPC INVERTER

Switching State								Output Voltage
Sa1	Sa2	Sa3	Sa4	Sb1	Sb2	Sb3	Sb4	Vab
1	1	0	0	0	0	1	1	V_{dc}
1	1	0	0	0	1	1	0	$\frac{V_{dc}}{2}$
0	1	1	0	0	0	1	1	
1	1	0	0	1	1	0	0	
0	1	1	0	0	1	1	0	0
0	0	1	1	0	0	1	1	
0	1	1	0	1	1	0	0	$-\frac{V_{dc}}{2}$
0	0	1	1	0	1	1	0	
0	0	1	1	1	1	0	0	$-V_{dc}$

On the other hand, in this study, SMC method, which is in the nonlinear controller group, was used for grid current control. The reference studies provide specifics on how to use the SMC control method for grid-connected inverter systems [26], [27]. The main idea of SMC is to bring the system state variables onto a pre-defined sliding surface through discontinuous control and to force them to move on this surface, and also to control them by approaching the origin point, as seen in Fig. 3. This concept requires the existence of a sliding surface and a control signal for its implementation. Generally, the sliding surface is constructed using state variable errors, and the sliding surface function, which is a linear combination of state variable errors, can be expressed as follows:

$$S(x) = \lambda x_1 + \dot{x}_1 \tag{1}$$

where $x_1$and $\dot{x}_1$ denote the state variable error and its derivative, respectively.λ is a positive constant called the sliding coefficient. The value of the sliding coefficient is a parameter that has an effect on the dynamic response of the system and should always be chosen as positive to ensure stability[27]. However, an excessively large λ value can jeopardize the stability of the system. Therefore, through trial and error and considering the switching frequency that determines the

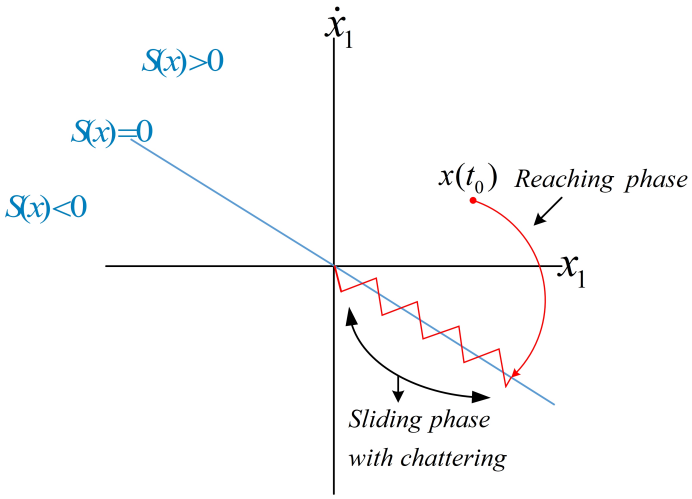

Fig. 3. Graphical explanation of sliding mode control.

dynamics of the system, λ has been chosen as 5000 in this study. In grid-connected inverter systems, the main purpose is to control grid current. Therefore, x_1 can be determined as the error $(i_g{}^* - i_g)$ of the grid current. In addition, in order to weaken the resonance problem in the LCL filter mentioned in the introduction, the sliding surface can also be formed with the capacitor voltage error $(v_c - v_c{}^*)$. The adjustment of capacitor voltage results in automatic adjustment of grid current as a natural consequence.After determining the sliding surface function, the control signal that forces the state variables to act on the sliding surface must be determined. The structure of the control signal can be expressed as in Eq. (2):

$$u_{smc} = u_{eq} + u_{sw} \tag{2}$$

where u_{eq} is the equivalent control signal that determines the system change on the sliding surface, and u_{sw} is the discontinuous switching control input that drives the state variables to the sliding surface and enforces the state variables to act on the sliding surface even in the presence of parameter changes and distortions. The equivalent control (u_{eq}) signal can be obtained by setting the derivative of the sliding surface function to zero $(\dot{S}(x) = 0)$. However, including the equivalent control part in the control signal increases overall computation time and control complexity [28]. Therefore, the use of a simpler discontinuous switching control signal is widely preferred [18], [27], [28]. In general, the discontinuous switching control signal connected to the sliding surface and with a control gain of 1 (one) can be expressed as in Eq. (3):

$$u_{smc} = u_{sw} = -\,\mathrm{s}\,ign(S(x)) = \begin{cases} +1 & if\ S(x) < 0 \\ -1 & if\ S(x) > 0 \end{cases} \tag{3}$$

where the sign() denotes the signum function [19], [23]. The chattering problem in practical applications can arise due to the discontinuous structure of the switching control signal, which switches between 1 and -1 values based on the sliding surface's sign [27]. As seen from Eq. (3), the control input is negative when the sliding surface is positive, and it is positive when the sliding surface is negative. Therefore, the control signal can be viewed as a switching function that changes its

value when the state variable's trajectory intersects the sliding surface. Furthermore, the chattering phenomenon observed in power converter applications has adverse impacts such as reduced control precision and power losses. Thus, minimizing chattering is crucial in SMC, and several techniques for reducing chattering have been proposed in literature [18], [20], [27]. One of the methods to reduce chattering is the boundary layer method. This method reduces chattering by passing the sliding surface function through a boundary layer of thickness ϕ. The signum function in the discontinuous switching control signal is then replaced by the $S(x)/\phi$ signal, which makes the control input continuous within the boundary layer and reduces chattering [26], [28]. As a result, the appropriate switching signals for the inverter are obtained by comparing the $S(x)/\phi$ signal with the triangle carriers.

A. Proportional-resonant (PR) control

The capacitor voltage reference ($v_c{}^*$) for the LCL filter connection state was successfully obtained using the excellent AC signal tracking capability of the PR control. The transfer function of the PR control is given in Eq. (4). When the grid current error is applied to the input of the transfer function, the output is $v_c{}^*$.

$$H_{PR}(s) = K_p + \frac{2K_r\omega_c s}{s^2 + 2\omega_c s + (2\pi f_g)^2} \tag{4}$$

where K_p is the proportional gain, K_r is the resonant gain, and w_c is the cut-off frequency. The dynamic and steady-state responses of the PR control are determined by adjusting the parameter values K_p and K_r. The derivation of proportional and resonant gains is analyzed in [23]. The gain values obtained according to the equations expressed in [23] are readjusted to improve the performance of the controller. Therefore, in this study, K_p and K_r were tuned to 3 and 1500, respectively. w_c is 1 rad/s.

III. L-TYPE FILTER DESIGN

Fig. 4 illustrates the circuit diagram of the L filter, which is placed between the inverter and the grid. The filter comprises of the filter inductance, denoted by L_i, and its internal resistance, r_i.

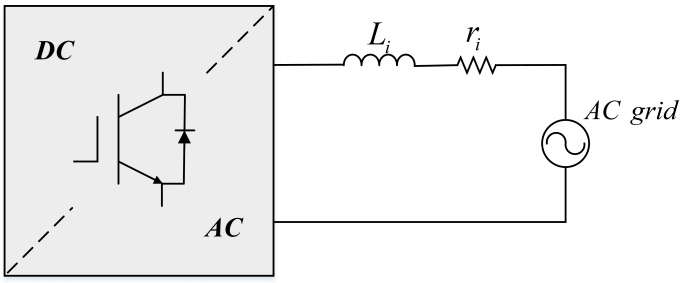

Fig. 4. L filter circuit diagram.

The inductance value (L_i) in the filter L can be determined by considering the current fluctuation on the inverter output side [16], [21]. The analysis of current ripple for all switch states of the inverter is a difficult task. Therefore, it is necessary to obtain an equation that provides the maximum current fluctuation value while considering the inverter structure. As the HNPC inverter transfers power to the grid, the input voltage is higher than the grid voltage, indicating that the HNPC inverter is a buck-type inverter. To determine the inductance value, the HNPC inverter can be simplified to a half-wave buck converter model at the switching frequency, as illustrated in Fig. 5 [17]. In this model, the neutral point of the inverter and the neutral point of the grid are short-circuited, and the grid has a half-sinusoidal waveform.

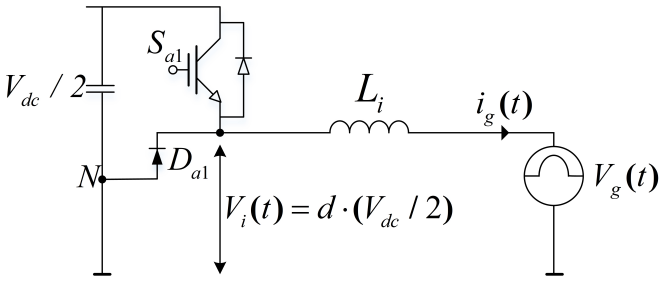

Fig. 5. Simplified HNPC inverter model.

The value of the inductance can be determined by using Eq. (5), which is derived from the analysis of the model in Fig. 5 in continuous current mode

$$L_i = \frac{\frac{V_{dc}}{2} - V_g}{2 \cdot \Delta I_L} \cdot \frac{d}{f_{sw}} \tag{5}$$

where d is the duty cycle, and the largest current ripple value (ΔI_L) occurs when the duty cycle is 50% [29]. Therefore, the inductance value is obtained as in Eq. (6).

$$L_i = \frac{\frac{V_{dc}}{2} - \frac{1}{2} \cdot \frac{V_{dc}}{2}}{2 \cdot \Delta I_L} \cdot \frac{1}{2 \cdot f_{sw}} = \frac{V_{dc}}{16 \cdot f_{sw} \cdot \Delta I_L} \tag{6}$$

The maximum amplitude value of the current ripple is calculated as in Eq. (7):

$$\Delta I_{L\max} = r \cdot \frac{P_i \cdot \sqrt{2}}{V_g} \tag{7}$$

where r denotes the ripple rate of the current transferred to the grid, and generally the current ripple rate is chosen as 10%–20% in LCL filter design [15], [30].

The L filter design process requires a balance between the need for a low value to maintain THD of the grid current within the limit set by international standards [31], and the need to avoid raising the inductance value too much, which would increase the filter size and cost. To strike this balance, the current ripple ratio was chosen as 10%, considering the impact of the inverter topology and control technique on the THD of the system. The system parameters used in the filter design are provided in Table 2. By using Eq. (6) and (7), the inductance value was calculated as $L_i = 3.85\,mH$.

TABLE II
SYSTEM PARAMETERS

Parameter	Value
Inverter output power (P_i)	$3\,kW$
DC bus voltage (V_{dc})	$500\,V$
Grid voltage amplitude (V_g)	$220\,V_{rms}$
Switching frequency (f_{sw})	$5\,kHz$

IV. LCL-TYPE FILTER DESIGN

The circuit diagram of the LCL filter placed between the inverter and the grid is shown in Fig. 6, where L_i denotes the inductance value on the inverter side, L_g denotes the inductance value on the grid side, and C_f denotes the filter capacitor. In addition, it symbolizes the r_i and r_g inductances' internal resistances.

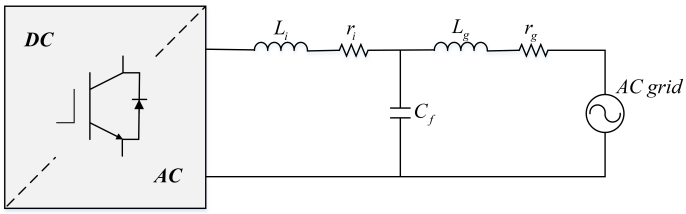

Fig. 6. LCL filter circuit diagram.

The inductance value on the inverter side is found with the help of Eq. (6) and (7). Considering the inductance value on the grid side, the current fluctuation rate was chosen as 20%.

While determining the filter capacitor value, the maximum power factor change acceptable by the grid is assumed to be 5%, and this value corresponds to 5% of the capacitor base value. Eq. (8) and (9) show the calculation of filter base values. The calculation of the filter capacitor value is given in Eq. (10).

$$Z_b = \frac{{V_g}^2}{P_i} \tag{8}$$

$$C_b = \frac{1}{2\pi f_g \cdot Z_b} \tag{9}$$

$$C_f = \%5 \cdot C_b \tag{10}$$

The inductance value on the grid side can be calculated using Eq. (11):

$$L_g = k \cdot L_i \tag{11}$$

where k denotes a constant correlation coefficient between the inverter and the grid-side inductances. This coefficient takes a value in the $0 < k \leq 1$ range, and usually a value of 1 or close to 1 can be selected in high power applications.

To ensure that the LCL filter effectively suppresses harmonic distortion within the switching frequency range, it is necessary to meet the requirement statedin Eqs. (12):

$$10 f_g \leq f_{res} \leq \frac{1}{2} f_{sw} \tag{12}$$

where f_{res} is the resonant frequency of the filter and is expressed by Eqs. (13) [32].

$$f_{res} = \frac{\sqrt{\frac{L_i + L_g}{L_i \cdot L_g \cdot C_f}}}{2\pi} \tag{13}$$

By using above equations, the inductors and capacitor values have been calculated as $L_i = 1.62\,mH, L_g = 0.6\,mH, C_f = 9.87\,\mu F$, and $f_{res} = 2422.28\,Hz$.

V. SIMULATION RESULTS

In order to evaluate the effectiveness of L and LCL filter topologies with single-phase HNPC inverters in mitigating harmonic distortion and their impact on grid current, a modeling study was carried out using MATLAB/Simulink®. The simulation utilized system parameters and calculated filter values, which are presented collectively in Table 3.

TABLE III
SYSTEM PARAMETERS.

Parameter	Value (L filter)	Value (LCL filter)
Inverter output power (P_i)	$3\,kW$	$3\,kW$
DC bus voltage (V_{dc})	$500\,V$	$500\,V$
Inverter-side inductance (L_i)	$3.85\,mH$	$1.62\,mH$
Grid-side inductance (L_g)	×	$0.6\,mH$
Filter capacitance (C_f)	×	$9.87\,\mu F$
Grid voltage amplitude (V_g)	$220\,V_{rms}$	$220\,V_{rms}$
Switching and grid frequencies (f_{sw}, f_g)	$5\,kHz, 50\,Hz$	$5\,kHz, 50\,Hz$
Sampling time (T_s)	$1\,\mu s$	$1\,\mu s$

Fig. 7 and 8 show MATLAB/Simulink®-based modeling of a single-phase grid-connected HNPC inverter circuit with L and LCL filters, respectively. In both models, the inverter topology (HNPC), switching technique (SPWM), and control method (SMC) are used similarly. In addition, as seen in Fig. 8, the control of the grid current with appropriate damping is provided by controlling the capacitor voltage. Therefore, proportional-resonant (PR) control, which has an excellent AC signal tracking feature, is used to generate the reference value of the capacitor voltage.

The waveforms of the grid voltage and current for both L and LCL filters are illustrated in Fig. 9. It can be observed that the current transferred to the grid experiences fewer fluctuations with an LCL filter connection as compared to an L filter connection. It is evident that in both filter topologies, the grid current follows a sinusoidal waveform and remains in-phase with the grid voltage. By aligning the grid current and voltage, the power factor can be improved such that it approaches or equals one, thereby decreasing the consumption of reactive power.

In the L and LCL filter connection states, the active power transferred to the grid with the fundamental frequency (50 Hz) component is shown in Fig. 10. In the case of an L filter connection, 2943 W of active power is transferred to the grid, while in the case of an LCL filter connection, 2954 W of active power is transferred. Both filter topologies result in nearly zero reactive power due to their design. The LCL filter provides superior harmonic attenuation, resulting in lower amplitudes of harmonic components (excluding the fundamental frequency)

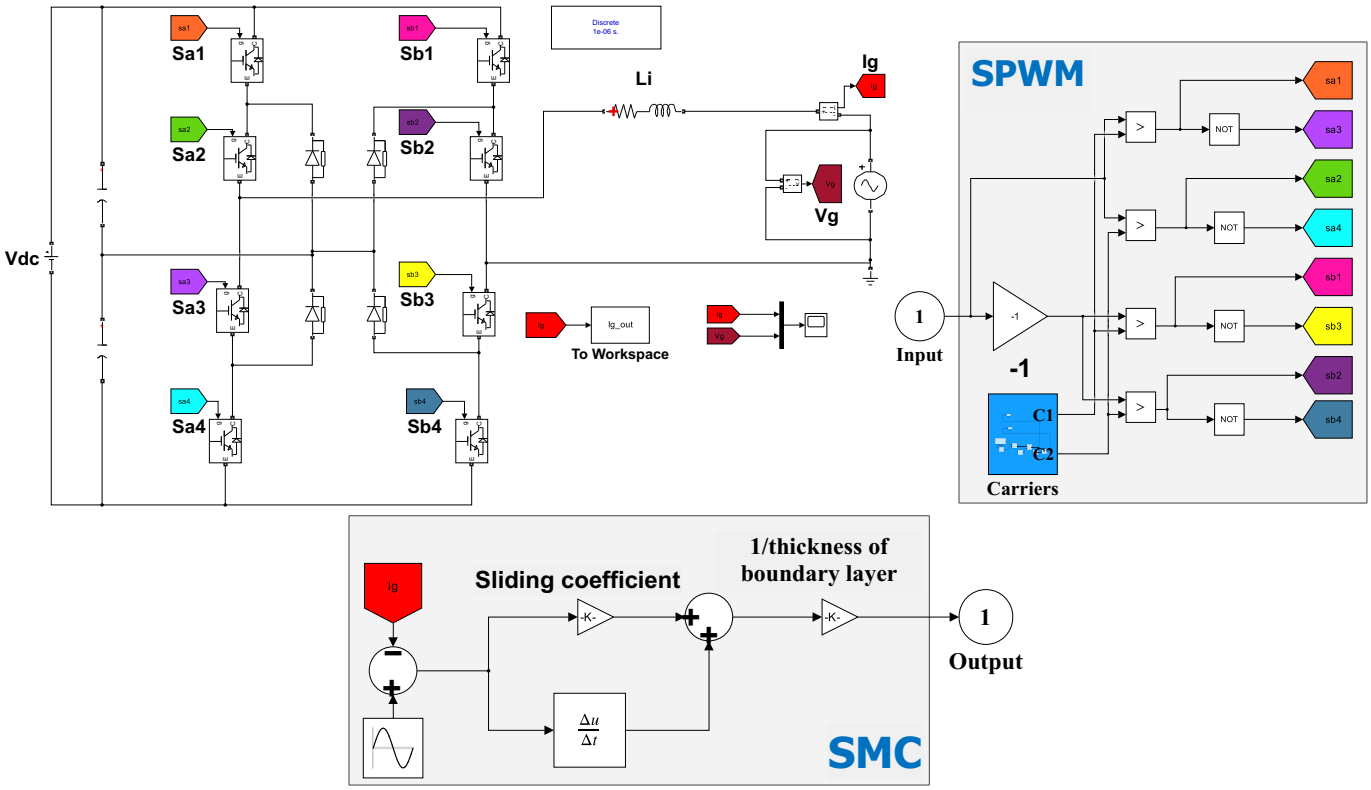

Fig. 7. L filter simulink model.

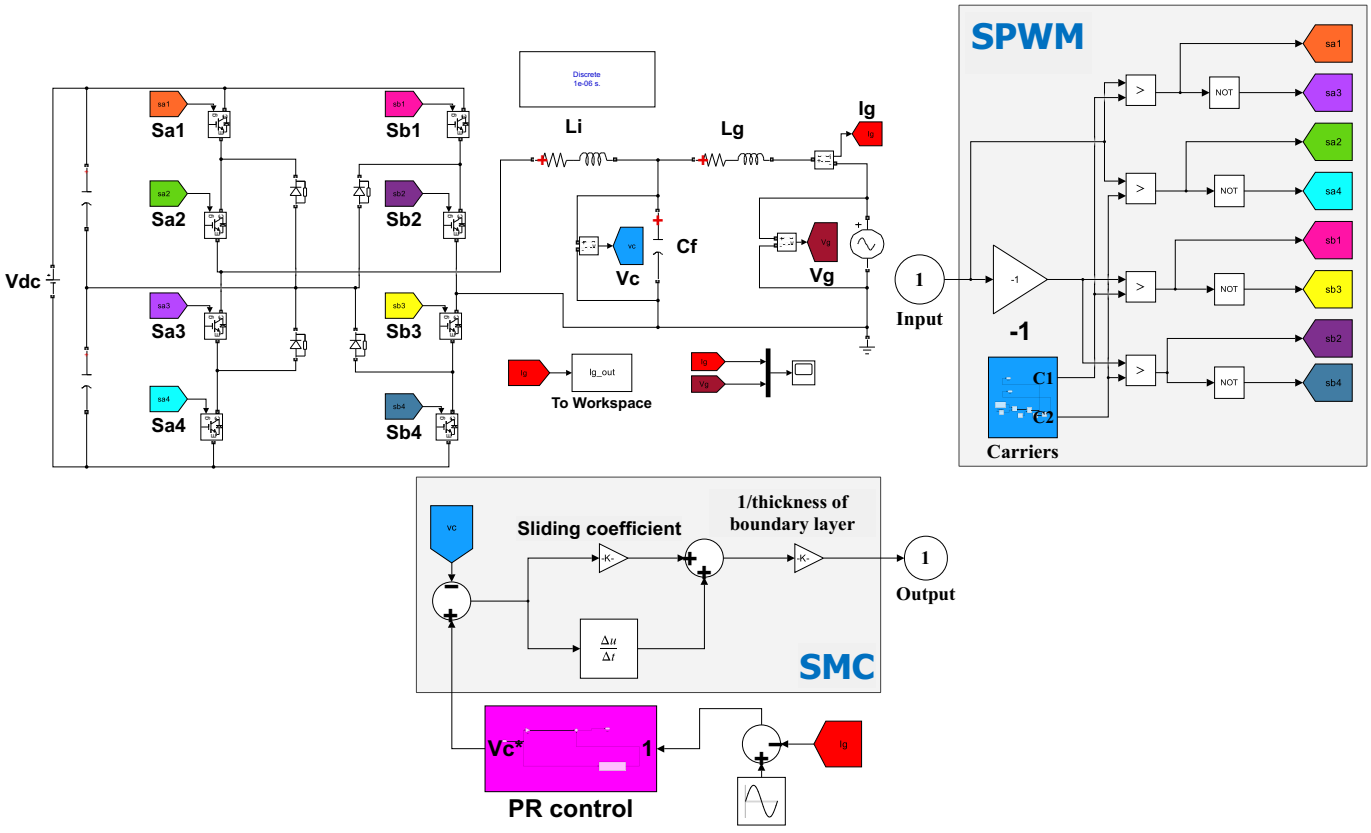

Fig. 8. LCL filter simulink model.

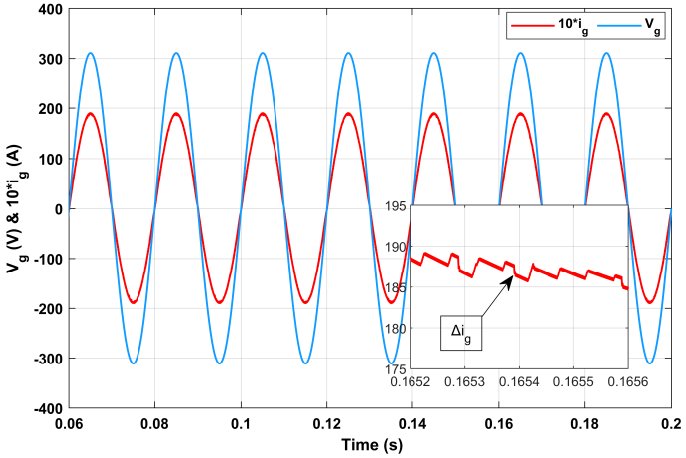

(a)

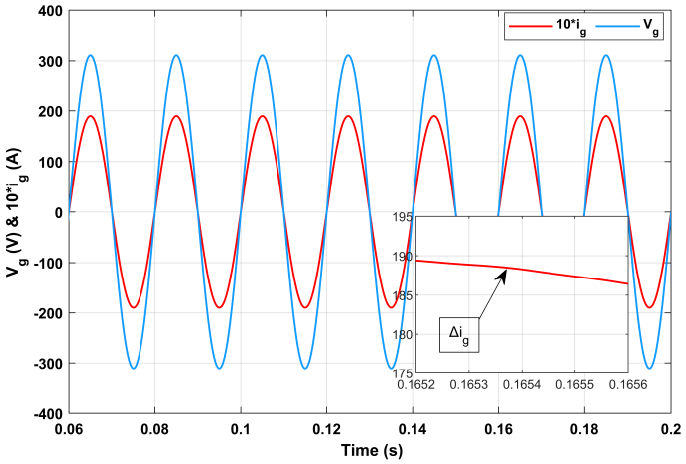

(b)

Fig. 9. Grid current and voltage waveforms a) for L filter b) for LCL filter.

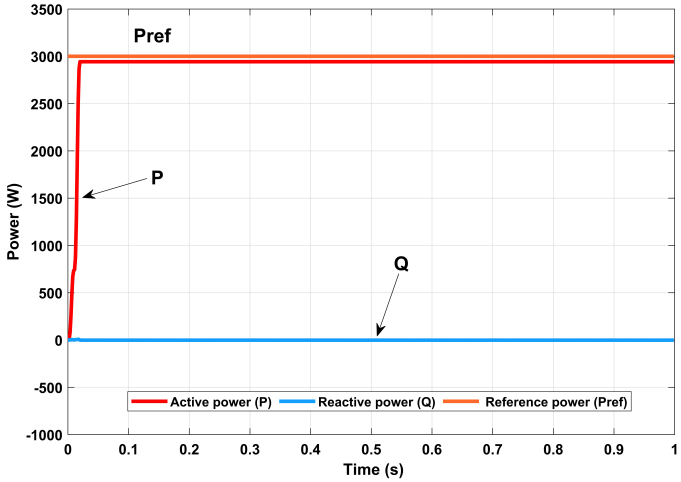

(a)

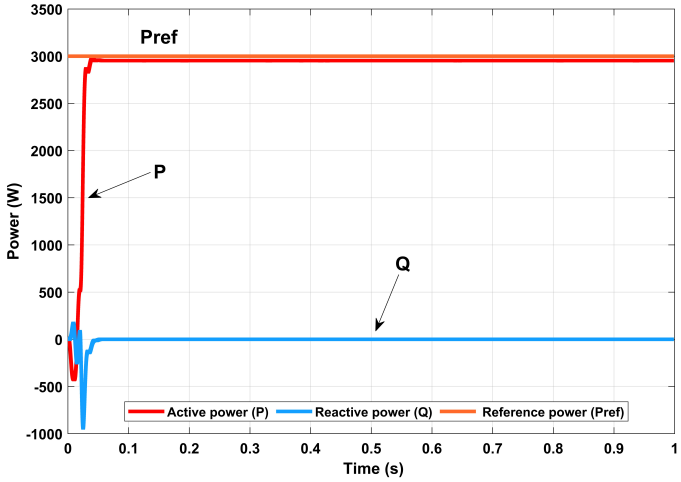

(b)

Fig. 10. Active power transferred to the grid a) for the L filter b) for the LCL filter.

and higher amplitudes of the fundamental frequency component. As a result, the LCL filter enables greater transmission of active power to the grid when compared to the L filter.

The FFT analysis tool in Power GUI was used to perform THD analysis of the grid current for both L and LCL connection states, and the results are presented in Fig. 11. The figure illustrates that the THD values of the grid current for L and LCL connection states are 1.56% and 0.07%, respectively. Moreover, it is apparent that the grid current in both cases, particularly with the LCL filter, consists of odd harmonic components, whose amplitudes are significantly smaller than those of the fundamental frequency components.

The comparison of L and LCL filters based on the obtained results is given in Table 4. Although LCL filters require an additional damping method or control of the capacitor voltage due to the resonance problem, they are seen to be advantageous in terms of harmonic attenuation, efficiency, and grid current fluctuation. In addition, the fact that they require a lower inductance value compared to L filters reduces power loss and contributes to the efficiency of the system.

TABLE IV
COMPARISON OF L AND LCL FILTERS.

Comparison category	L filter	LCL filter
Harmonic attenuation performance	Good	Very good
Current fluctuation	Acceptable	Low
Resonance damping	Not applicable	Naturally
THD value of grid current	1.56%	0.07%
Inverter efficiency	98.1%	98.46%

VI. CONCLUSION

In this study, two filter topologies, L and LCL, commonly used in grid-connected renewable energy systems, were an-

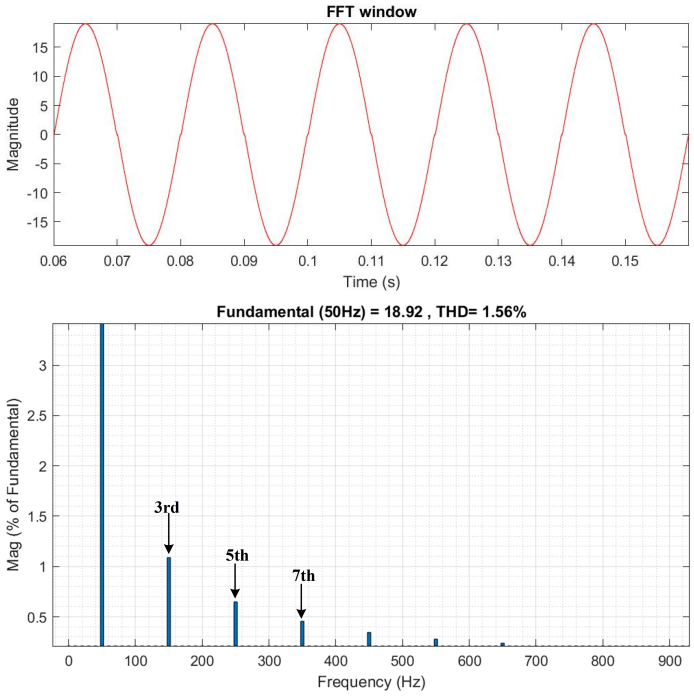

(a)

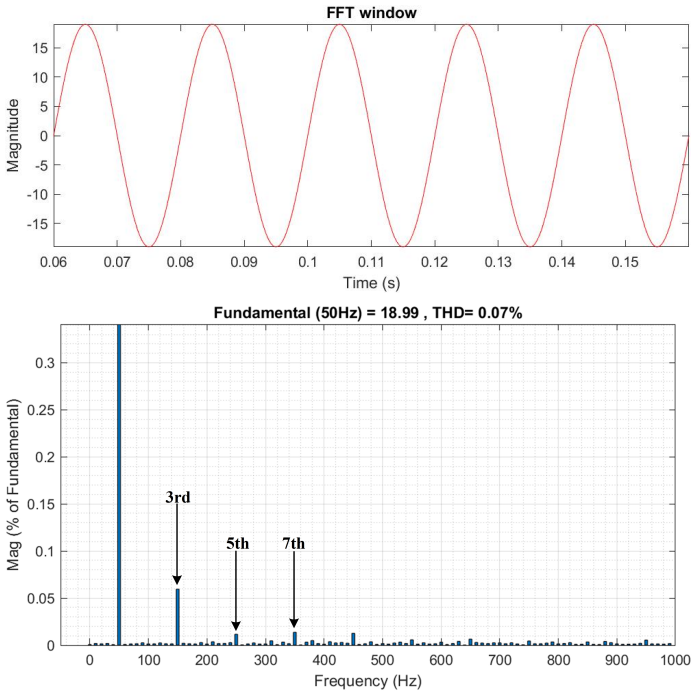

(b)

Fig. 11. Grid current THD analysis a) for L filter b) for LCL filter.

alyzed.Both filter topologies were designed for the HNPC inverter, and their harmonic attenuation performances were compared, along with their effects on the current and power transferred to the grid. In order to make the analysis more realistic, all components (inverter topology, switching technique, control method, parameters used in the control method, simulation configuration) that could affect the results were kept similar in both filter types. The simulation results showed that the THD value of the grid current was within the limits specified by international standards (IEEE 1547, IEC 61727) for both filter topologies. However, the LCL filter exhibited better harmonic attenuation performance with a lower inductance value compared to the L filter. In addition, the LCL filter provided lower current fluctuation and allowed more active power transfer to the grid. The resonance problem in the LCL filter is naturally dampened by controlling the capacitor voltage without the need for an additional damping method. Furthermore, the grid current was successfully controlled via the control of the capacitor voltage. The HNPC inverter used in this study has a multi-level output, which inherently results in a lower THD value compared to other inverter topologies. As a result, with the use of a suitable control method, it can be applied in an L filter topology that does not require a high inductance value, while still ensuring that the THD value remains within the limits specified by international standards.

The study does not provide a detailed description of the control method. In future work, a comprehensive analysis of the entire system and the grid current will be conducted, along with a thorough explanation of the control method.

REFERENCES

[1] I. E. Agency, *World Energy Outlook 2022*, 2022.

[2] F. Blaabjerg, D. M. Ionel, Y. Yang, and H. Wang, "Renewable energy systems: Technology overview and perspectives," *Renewable Energy Devices and Systems with Simulations in MATLAB® and ANSYS®*, pp. 1–16, 2017.

[3] I. R. E. Agency, *Future of Solar Photovoltaic: Deployment, investment, technology, grid integration and socio-economic aspects (A Global Energy Transformation: paper)*, 2019.

[4] H. Noh, K. Kang, and Y. Seo, "Environmental and energy efficiency assessments of offshore hydrogen supply chains utilizing compressed gaseous hydrogen, liquefied hydrogen, liquid organic hydrogen carriers and ammonia," *International Journal of Hydrogen Energy*, vol. 48, no. 20, pp. 7515–7532, 2023.

[5] M. H. Mohamed Hariri, M. K. Mat Desa, S. Masri, and M. A. A. Mohd Zainuri, "Grid-connected pv generation system—components and challenges: A review," *Energies*, vol. 13, no. 17, 2020.

[6] I. Sefa and N. Altin, "Grid interactive photovoltaic inverters-a review," *Journal of the Faculty of Engineering and Architecture of Gazi University*, vol. 24, no. 3, 2009.

[7] S. Kouro, J. I. Leon, D. Vinnikov, and L. G. Franquelo, "Grid-connected photovoltaic systems: An overview of recent research and emerging pv converter technology," *IEEE Industrial Electronics Magazine*, vol. 9, no. 1, pp. 47–61, 2015.

[8] M. İnci and Ömer Türksoy, "Review of fuel cells to grid interface: Configurations, technical challenges and trends," *Journal of Cleaner Production*, vol. 213, pp. 1353–1370, 2019.

[9] M. Obi and R. Bass, "Trends and challenges of grid-connected photovoltaic systems – a review," *Renewable and Sustainable Energy Reviews*, vol. 58, pp. 1082–1094, 2016.

[10] N. Rasekh and M. Hosseinpour, "Lcl filter design and robust converter side current feedback control for grid-connected proton exchange membrane fuel cell system," *International Journal of Hydrogen Energy*, vol. 45, no. 23, pp. 13 055–13 067, 2020.

[11] T. Duman, S. Marti, M. A. Moonem, A. A. R. Abdul Kader, and H. Krishnaswami, "A modular multilevel converter with power mismatch control for grid-connected photovoltaic systems," *Energies*, vol. 10, no. 5, 2017.

[12] E. Kabalcı, "Review on novel single-phase grid-connected solar inverters: Circuits and control methods," *Solar Energy*, vol. 198, pp. 247–274, 2020.

[13] X. Ruan, X. Wang, D. Pan, D. Yang, W. Li, and C. Bao, *Control techniques for LCL-type grid-connected inverters*. Springer, 2018.

[14] C. Gurrola-Corral, J. Segundo, M. Esparza, and R. Cruz, "Optimal lcl-filter design method for grid-connected renewable energy sources," *International Journal of Electrical Power Energy Systems*, vol. 120, p. 105998, 2020.

[15] M. Liserre, F. Blaabjerg, and S. Hansen, "Design and control of an lcl-filter-based three-phase active rectifier," *IEEE Transactions on Industry Applications*, vol. 41, no. 5, pp. 1281–1291, 2005.
[16] Y. Kim, H. Cha, B.-M. Song, and K. Y. Lee, "Design and control of a grid-connected three-phase 3-level npc inverter for building integrated photovoltaic systems," in *2012 IEEE PES Innovative Smart Grid Technologies (ISGT)*, 2012, pp. 1–7.
[17] S. V. Araujo, A. Engler, B. Sahan, and F. L. M. Antunes, "Lcl filter design for grid-connected npc inverters in offshore wind turbines," in *2007 7th Internatonal Conference on Power Electronics*, 2007, pp. 1133–1138.
[18] F. Sebaaly, H. Vahedi, H. Y. Kanaan, N. Moubayed, and K. Al-Haddad, "Sliding mode fixed frequency current controller design for grid-connected npc inverter," *IEEE Journal of Emerging and Selected Topics in Power Electronics*, vol. 4, no. 4, pp. 1397–1405, 2016.
[19] H. Komurcugil, S. Ozdemir, I. Sefa, N. Altin, and O. Kukrer, "Sliding-mode control for single-phase grid-connected LCL-filtered vsi with double-band hysteresis scheme," *IEEE Transactions on Industrial Electronics*, vol. 63, no. 2, pp. 864–873, 2016.
[20] S. Ozdemir, N. Altin, H. Komurcugil, and I. Sefa, "Sliding mode control of three-phase three-level two-leg npc inverter with lcl filter for distributed generation systems," in *IECON 2018 - 44th Annual Conference of the IEEE Industrial Electronics Society*, 2018, pp. 3895–3900.
[21] A. Reznik, M. G. Simões, A. Al-Durra, and S. M. Muyeen, "*lcl* filter design and performance analysis for grid-interconnected systems," *IEEE Transactions on Industry Applications*, vol. 50, no. 2, pp. 1225–1232, 2014.
[22] Y. Jia, J. Zhao, and X. Fu, "Direct grid current control of lcl-filtered grid-connected inverter mitigating grid voltage disturbance," *IEEE Transactions on Power Electronics*, vol. 29, no. 3, pp. 1532–1541, 2014.
[23] N. Altin, S. Ozdemir, H. Komurcugil, and I. Sefa, "Sliding-mode control in natural frame with reduced number of sensors for three-phase grid-tied lcl-interfaced inverters," *IEEE Transactions on Industrial Electronics*, vol. 66, no. 4, pp. 2903–2913, 2019.
[24] Y. Yang and F. Blaabjerg, "Overview of single-phase grid-connected photovoltaic systems," in *Renewable Energy Devices and Systems with Simulations in MATLAB® and ANSYS®*. CRC Press, 2017, pp. 41–66.
[25] T. Duman and M. Cengiz, "Comparative analysis of thd performances of different carrier based pwm techniques for single phase 5-level npc multilevel inverter." in *International Conference on Innovative Academic Studies (ICIAS 2022)*, 2022, pp. 937–944.
[26] S. Bayhan and H. Komurcugil, "A sliding-mode controlled single-phase grid-connected quasi-z-source npc inverter with double-line frequency ripple suppression," *IEEE Access*, vol. 7, pp. 160 004–160 016, 2019.
[27] H. Komurcugil, S. Biricik, S. Bayhan, and Z. Zhang, "Sliding mode control: Overview of its applications in power converters," *IEEE Industrial Electronics Magazine*, vol. 15, no. 1, pp. 40–49, 2021.
[28] F. Bagheri, H. Komurcugil, O. Kukrer, N. Guler, and S. Bayhan, "Multi-input multi-output-based sliding-mode controller for single-phase quasi-z-source inverters," *IEEE Transactions on Industrial Electronics*, vol. 67, no. 8, pp. 6439–6449, 2020.
[29] R. W. Erickson and D. Maksimovic, *Fundamentals of power electronics*. Springer Science Business Media, 2007.
[30] P. Gakhar and M. Gupta, "Harmonic mitigation in a transformer less grid connected solar pv system using modified lcl filter," in *2018 3rd International Conference and Workshops on Recent Advances and Innovations in Engineering (ICRAIE)*, 2018, pp. 1–4.
[31] A. Karafil, "Tek fazlı Şebeke bağlantılı eviricilerde l, lcl ve llcl tipi filtre tasarımı[design of l, lcl and llcl type filter for single phase grid connected inverters]," *Karadeniz Fen Bilimleri Dergisi*, vol. 12, no. 1, pp. 448 – 460, 2022.
[32] K. A. El Wahid Hamza, H. Linda, and L. Cherif, "Lcl filter design with passive damping for photovoltaic grid connected systems," in *IREC2015 The Sixth International Renewable Energy Congress*, 2015, pp. 1–4.

Muhammet Cengiz was born in Erzurum, Turkey, in 1994. In 2018, he graduated from Erzurum Atatürk University with a bachelor's degree in Electrical and Electronics Engineering. He is currently a master's student at Erzurum Technical University's Department of Electrical and Electronics Engineering and has been working as a research assistant in the same department since 2022. His current research interests include power electronics, multilevel power converters, sliding mode control, and renewable energy systems.

Turgay Duman was born in Erzurum located in the eastern region of Turkey. He studied Electrical and Electronic Engineering and earned a Bachelor's degree in Engineering from Ataturk University in 2010. He worked as an Electrical Engineer at Information Technologies and Communication Authority in 2011 in Erzurum, Turkey. He recieved his Master's and Ph.D degrees in Electrical Engineering from The University of Texas at San Antonio in 2014 and 2019, respectively. His research areas include power electronics, renewable energy systems, multilevel power converters, real-time simulations, and large sacale PV systems. He is currently working as an assistant professor at Erzurum Technical University.